Available online at www.sciencedirect.com
SCIENCE DIRECT
Polymer 46 (2005) 2699–2709
polymer
www.elsevier.com/locate/polymer

Heterogeneous crosslinking of waterborne two-component polyurethanes (WB 2K-PUR); stratification processes and the role of water

Daniel B. Otts, Marek W. Urban*

Shelby F. Thames Polymer Science Research Center, School of Polymers and High Performance Materials, The University of Southern Mississippi, 118 College Drive # 10076, Hattiesburg, MS 39406, USA

Received 22 October 2004; accepted 6 January 2005

Abstract

Stoichiometric imbalance and crosslinking conditions during film formation of waterborne two-component polyurethanes (WB 2K-PUR) play a significant role in the development of material properties. Changing isocyanate-to-hydroxyl (NCO:OH) ratios from 1.0 to 2.2 over a range of humidities significantly affects film morphology, and these studies show that while films with higher NCO:OH exhibit increased T_g and surface roughness when crosslinked at high RH, a T_g decrease is observed at elevated RH. Higher RH conditions not only result in increased urea and decreased urethane content, but also facilitate enrichment of poly(ethylene glycol) (PEG) functionality near the film–air (F–A) interface due to stratification of PEG-modified polyisocyanate crosslinkers. Reaction-induced stratification also occurs during film formation resulting in the T_g differences between F–A and F–S interfaces: namely $T_{g,F-A} > T_{g,F-S}$ at 32 and 52%RH, whereas $T_{g,F-A} \leq T_{g,F-S}$ at 75%RH, as determined by interfacial micro thermal analysis (μTA). This behavior is attributed to concentration gradients of water during film formation and their corresponding effects on isocyanate hydrolysis reactions in conjunction with PEG stratification near the F–A interface. Furthermore, excessive stoichiometric NCO:OH imbalance results in the formation of microscopic 'hills' and 'valleys' on the F–A surface having T_g differences of 6 °C. These phenomenological processes are incorporated into a model describing WB 2K-PUR film formation as a function of crosslinking conditions and resulting morphological features.

Keywords: Water-borne polyurethanes; FT-IR; Film formation

1. Introduction

Polyurethanes (PUR's) represent a versatile class of polymers due to numerous structural features resulting in many useful and intriguing properties. One of unique attributes of PURs is their morphology, which may be carefully tailored with appropriate selection of starting materials and their formulation. In fact, significant knowledge exists regarding bulk and surface morphological development in PUR's and one of the key features is the development of phase separated systems in which urethane-rich and urea-rich domains co-exist. Such heterogeneous morphologies may result from reaction-induced phase separation [1], thermodynamic incompatibility between soft and hard segments in PUR block copolymers [2,3], or by incorporation of fluorinated [4–6] and/or surface-active moieties [7], to name a few. Several excellent studies have capitalized on the high atomic force microscopy (AFM) resolution offered by tapping mode to investigate surface morphology, spatial distribution, and microstructural order of heterophases in PURs [2–5,7,8]. Furthermore, high-resolution near edge X-ray absorption spectroscopy (NEXAFS) has been utilized to directly observe and quantify the extent of urethane/urea phase separation in water-rich PUR plaques based on block copolymer formulations used for water-blown flexible PUR foams [9].

Although, numerous studies have been conducted on the structure–property relationships of thermoplastic and thermosetting PUR systems, only sporadic and limited knowledge exists concerning morphology development of their waterborne counterparts [10–22]. In fact, of the studies pertaining to PUR materials synthesized in or prepared from

* Corresponding author. Tel.: +1 601 2666454; fax: +1 601 2665504.
E-mail address: marek.urban@usm.edu (M.W. Urban).

0032-3861/$ - see front matter © 2005 Elsevier Ltd. All rights reserved.
doi:10.1016/j.polymer.2005.01.053

aqueous environments, a significant amount of research has focused on polyurethane dispersions (PUD's) [21–23], which are stable colloidal dispersions of thermoplastic or crosslinked polyurethane particles. However, from an application standpoint, crosslinked PUR's provide a number of advantages such as chemical resistance, improved mechanical properties, and durability that are not achievable with thermoplastic materials. Waterborne two-component polyurethanes (WB 2K-PUR) [10–20,24] represent an extremely useful class of thermosetting PUR materials in terms of their advantageous properties and attractiveness resulting from the reduction of volatile organic compounds (VOC's) during film formation. However, the inherent sensitivity of WB 2K-PUR systems to a number of physico-chemical variables including temperature, humidity, film thickness, and reactant stoichiometry can significantly alter a number of critical film properties, such as glass transition temperature (T_g), surface morphologies, and mechanical properties, to name a few [16,20]. Such process-driven complexities can make identification of molecular-level mechanisms responsible for morphological development exceedingly difficult.

Hydrophilic modification of conventional polyisocyanates has been used to facilitate water dispersibility by incorporation of short mono-functional methoxy-terminal poly(ethylene glycol) (PEG) chains through reactions with a fraction of the isocyanate groups of the crosslinker [14,16,25], and the reaction product of hexamethylene diisocyanate (HDI) trimer with mono-functional PEG shown below serves as a representative structure for water-dispersible polyisocyanates (WDPI). Such hydrophilic modifications lead to a complex solution morphology of WB 2K-PUR systems, which contain heterogeneously dispersed polyisocyanate droplets, water, and polyol, along with other ancillary components [10]. During film formation of such reactive dispersions, the question is what are molecular level mechanisms that govern this process? Despite the aforementioned inherent complexities, a significant amount of fundamental scientific and practical knowledge pertaining to WB 2K-PUR's has been realized in recent years. For example, high humidity conditions have been shown to increase the rate of isocyanate (NCO) consumption during film formation [15]. The same studies also suggested formation of concentration gradients of NCO functionalities across the film thickness during crosslinking, as evidenced by differing rates of isocyanate consumption at film–air (F–A) and film–substrate (F–S) interfaces. Heterogeneous film formation has also been observed in WB 2K-PUR's as a result of phase separation of polyurethane and polyurea [19]

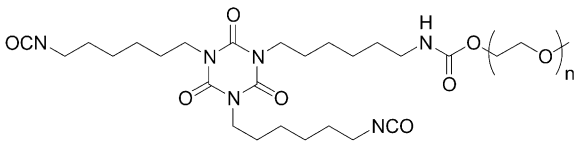

as well as uneven crosslinker distribution [17,18]. In the context of these studies, it also became evident that molecular level probes are essential in order to fully understand WB 2K-PUR film formation [26,27].

Although, the film formation of WB 2K-PUR has been the object of previous studies [13,15,20], it is an undisputedly complex combination of water evaporation, reactant coalescence, diffusion, and crosslinking reactions which requires further study. The present studies focus on a zero-VOC WB 2K-PUR system consisting of PEG-modified water dispersible polyisocyanate of HDI and a polyester polyol resin aqueous dispersion containing pendant carboxylic acid groups. The ultimate goal of these studies is to correlate specific physical surface morphological features with molecular level processes governing film formation.

2. Experimental section

Polyurethane/urea films were prepared by mixing Bayhydrol XP-7093 (Bayer Corp.) polyester polyol resin dispersion (approx. 30% w/w solids in water) with neat Bayhydur 302 (Bayer Corp.) water-dispersible polyisocyanate crosslinker based on PEG-modified polyisocyanate of HDI using overhead agitation at 1800 rpm with a small 4-blade PTFE impeller in a 20 ml glass vial at 25 °C for 10 min. The relative amounts of all components were adjusted to yield isocyanate to hydroxyl (NCO:OH) molar equivalent ratios ranging from 1.0 to 2.2, while maintaining 50% w/w solids. Following the mixing process, such mixture was held without agitation for 15 min to allow for viscosity reduction. Such mixture was applied to obtain approx. 40 μm (±3 μm) thick films (dry) on glass after crosslinking for 3 days in controlled environments at 30 °C and 32, 52, 75 and 82% relative humidities (%RH).

Differential scanning calorimetry (DSC) measurements were performed on a TA Instruments DSC Q100 using an initial heating rate of 20 °C/min from 40 to 150 °C followed by cooling at 20 °C/min to −50 °C to establish thermal history and to remove water from each specimen. A second scan was performed over the temperature range of −50 to 100 °C using modulated DSC with a heating rate of 3 °C/min, a modulation amplitude of 2 °C, and modulation period of 40 s. Attenuated total reflectance Fourier transform infrared (ATR-FTIR) spectra were obtained using a Digilab FTS 6000 system with a Ge ATR crystal (Pike Technologies) at a 45° angle of incidence, providing a penetration depth of approx. 600 nm. Contact mode atomic force microscopic (AFM) images were obtained using a TA Instruments Micro Thermal Analyzer 2990 which incorporates a Thermo Microscopes Explorer model AFM. Topographic images were acquired using scan rates ranging from 50 to 200 μm/s using silicon nitride contact AFM probes. AFM images were analyzed using ImageJ software [28] with a roughness calculation algorithm to determine root-mean-squared (RMS) surface roughness values. Additional scanning thermal microscopy (SThM) imaging was

performed using a Wollaston wire thermal probe having a constant temperature of 70 °C. Localized thermal mechanical analysis (LTA) was conducted using temperature ramps of 25 °C/s over the range of 20–100 °C. Reported LTA values represent average values calculated from approx. 24 individual LTA measurements. Standard deviations from such measurements were typically less than 2 °C. ^{1}H NMR spectra were acquired on a 500 MHz Varian INOVA spectrometer in DMSO-d_6 (Aldrich, 99.9 atom %D) using the following parameters: 45° pulse angle, 1.00 s relaxation delay, 1.891 s acquisition time.

3. Results and discussion

As a fist step, let us consider the effect of reactant stoichiometry on bulk thermal properties of WB 2K-PUR films, which was examined using modulated differential scanning calorimetry (MDSC). Fig. 1 shows a plot of glass transition temperature (T_g) as a function of NCO:OH ratio for selected RH conditions during crosslinking. As seen, an increase of the NCO:OH ratio results in a higher T_g for a given humidity, presumably due to greater extents of crosslinking and hydrogen bonding from urethane/urea groups [29]. Furthermore, the T_g decreases with increasing RH at each NCO:OH ratio, which is due to greater extents of isocyanate hydrolysis during film formation. Furthermore, the T_g's resulting from different %RH at each NCO:OH ratio also appear to converge to the same value with increasing NCO:OH ratios, which is most likely indicative of complete consumption of hydroxyl groups on polyol chains. It is also noteworthy that there was no evidence of multiple thermal transitions, consequently indicating no major bulk phase separation. Thus, RH as well as stoichiometric imbalance has a significant effect on crosslinking efficiency resulting in T_g values ranging from 12 to 34 °C.

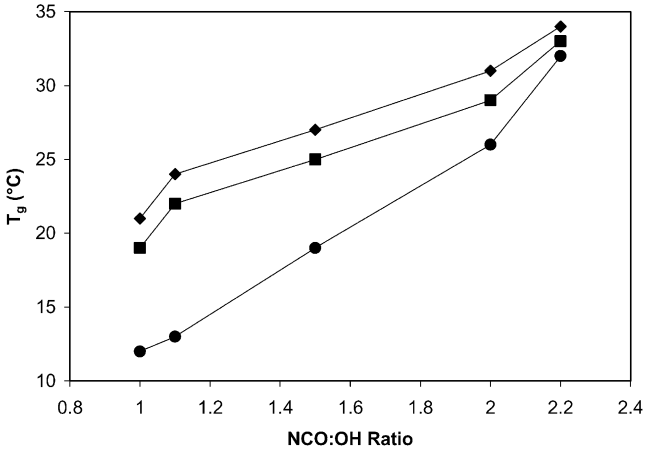

Fig. 1. Glass transition temperatures (T_g) of WB 2K-PUR films as a function of NCO:OH ratio for selected relative humidities during crosslinking at 30 °C. ♦ 32%RH; □, 52%RH; ●, 75%RH.

During the course of these studies it was observed that, when higher NCO:OH ratios were employed, visibly hazy films were produced when crosslinking was conducted at elevated RH. In an effort to identify morphological features responsible for haze formation, AFM images of films at the film–air (F–A) interface crosslinked at 82 and 75%RH with various NCO:OH ratios were acquired and are shown in Figs. 2 and 3, respectively. These images illustrate that with increasing NCO:OH ratio, larger, more irregular surface features are present, and the overall scale of surface morphological features is also larger for specimens crosslinked at 82%RH, as evidenced by the *z*-axis values of approximately 300 and 70 nm in Figs. 2 and 3, respectively.

In an effort to quantify morphological features AFM images in Figs. 2 and 3 were analyzed, and the relationship between root-mean-squared (RMS) surface roughness values and NCO:OH ratios was derived. This is shown in Fig. 4, which shows that there is an exponential increase of RMS surface roughness value with increasing NCO:OH ratio for PUR films crosslinked at 82%RH and 30 °C. However, the RMS roughness values of specimens crosslinked at 75%RH increase only slightly.

With these data in mind, let us consider chemical changes in crosslinked films with different NCO:OH ratios and RH conditions. As a next step, we collected ATR-FTIR spectra of PUR films with varied NCO:OH ratios crosslinked at 32, 52 and 75%RH. These spectra are shown in Fig. 5, Traces A–E, and reveal relevant features at 1724 and 1681 cm^{-1} due to ester groups of polyol resin and isocyanurate groups of polyisocyanate crosslinker [15], respectively, which vary significantly relative to each other as a function of NCO:OH ratio. A similar trend is observed when comparing the relative intensities of the bands at 766 and 732 cm^{-1} associated with in phase $-CH_2-$ rocking vibrations of HDI-based polyisocyanate crosslinker and out-of-plane aromatic C–H bending vibrations of polyol [30] Although, the observed spectral changes provide information concerning compositional variations, they provide little pertinent information about crosslinking reactions. Consequently, it is desirable to examine regions of the infrared spectrum where little or no band overlap from separate components exists. For this reason, we focused on the 1500–1600 cm^{-1} region associated with N–H bending vibrations [30] of urethane and urea functional groups. As seen in Fig. 5, the N–H bending region contains a broad, medium intensity band which is actually composed of two overlapping bands at approx. 1560 and 1524 cm^{-1} due to urea and urethane N–H bending vibrations, respectively, which was previously reported [12,31,32]. For each spectral overlay in Fig. 5, Traces A–E, higher RH specimens exhibit increased intensities of the 1560 cm^{-1} portion of the N–H bending band with a concomitant decrease at 1524 cm^{-1}. Furthermore, by normalizing all spectra to the 1681 cm^{-1} band associated with isocyanurate C=O stretching vibrations, relative extents of urethane and urea formation

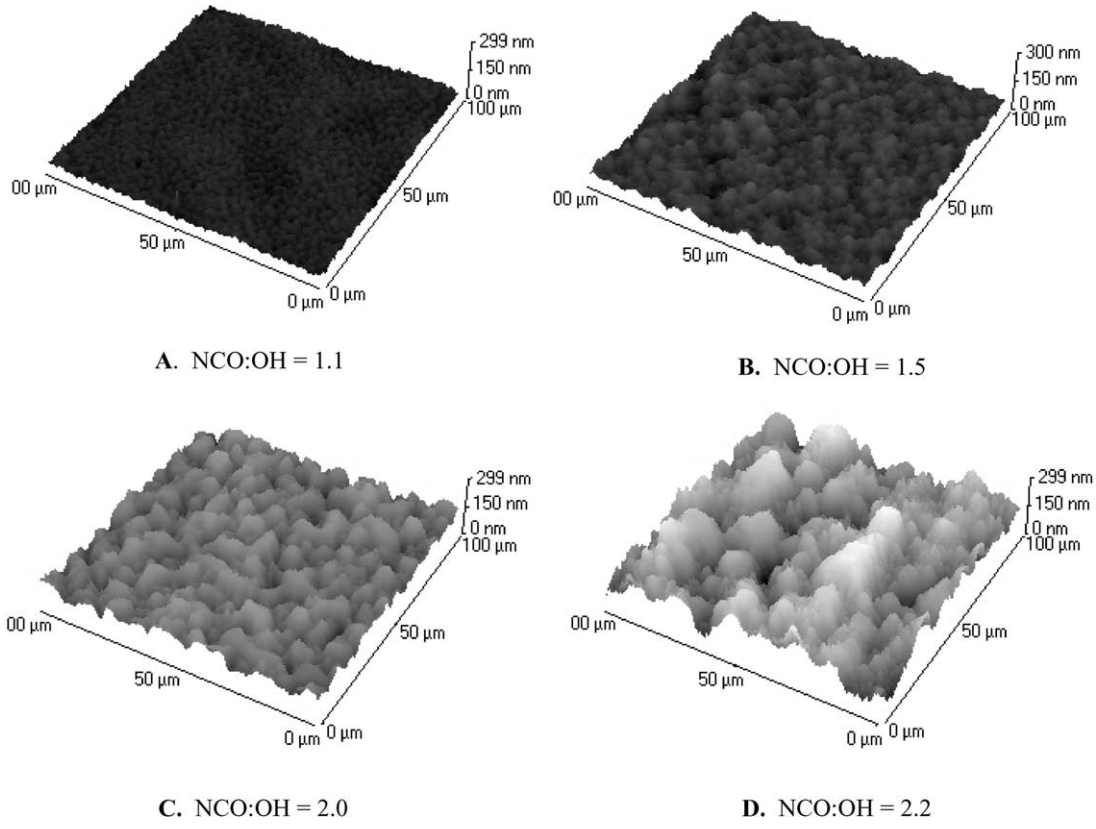

Fig. 2. Topographic AFM images of WB 2K-PUR films crosslinked at 82%RH and 30 °C with varying stoichiometries recorded from the film–air interface.

for various reaction conditions can be monitored by constructing absorbance profiles, such as those shown in Fig. 6. As seen in Fig. 6, the relative amount of urea increases with increasing RH as well as increased NCO:OH ratio, as evidenced by the 1560 cm^{-1} absorbance profile. This is attributed to the delayed evaporation of water due to higher ambient humidity levels during crosslinking, which will promote isocyanate hydrolysis reactions, ultimately leading to urea formation. Furthermore, such consumption of isocyanate groups due to hydrolysis limits urethane formation, as evidenced by the decrease in the 1524 cm^{-1} absorbance profile with increasing RH. The effect of NCO:OH ratio is also observed, with higher NCO:OH ratios resulting in both higher urea and urethane concentrations at each humidity, relative to the 1681 cm^{-1} band. Since both urea and urethane functional groups are products of crosslinking reactions, higher NCO:OH ratios lead to higher urea and urethane contents, as hydrolysis reactions of polyisocyanates leading only to amine (not urea) formation are minimized.

While Fig. 5 clearly illustrates spectral changes in the N–H bending region related to urea and urethane formation, there are also spectral changes in the 1000–1200 cm^{-1} region resulting from different RH conditions during crosslinking. Specifically, spectroscopic data obtained from films exposed to 32 and 52%RH crosslinking conditions in Fig. 5, Traces A–E, are identical in this region, whereas the 75%RH Trace in each group displays greater absorbance at approximately 1100 cm^{-1}. This difference becomes even more pronounced with the increasing NCO:OH ratio.

To investigate this phenomenon, Trace E in Fig. 5 was utilized to calculate a difference spectrum by subtracting the 52%RH spectrum from the 75%RH spectrum. This is shown in Fig. 7, Trace A, along with the ATR-FTIR spectrum of pure poly(ethylene glycol) (PEG, Aldrich, $M_n = 400$ g/mol) in Trace B. A comparison of these two spectra reveal striking similarities, specifically with regard to the band at 1100 cm^{-1} associated with asymmetric C–O–C stretching vibrations of ether groups [30]. Similarly, the bands at 1350, 1462 and 3445 cm^{-1} are detected in both spectra. Close inspection of the difference spectrum in Trace A reveals bands at 1647 and 1560 cm^{-1} which are associated with C═O stretching and N–H bending vibrations due to urea, respectively. Furthermore, the band at 1697 cm^{-1} most likely results from urethane and/or allophanate C═O stretching vibrations, which are functional groups typically used to anchor PEG moieties to HDI-based polyisocyanate crosslinkers, thereby imparting water-dispersibility [25]. Based on these observations, increased %RH during crosslinking facilitates enrichment of PEG-containing structural units near the F–A interface. It should also be pointed out that the simultaneous increase of the band intensities at 1100, 1560 and 1647 cm^{-1} near the F–A

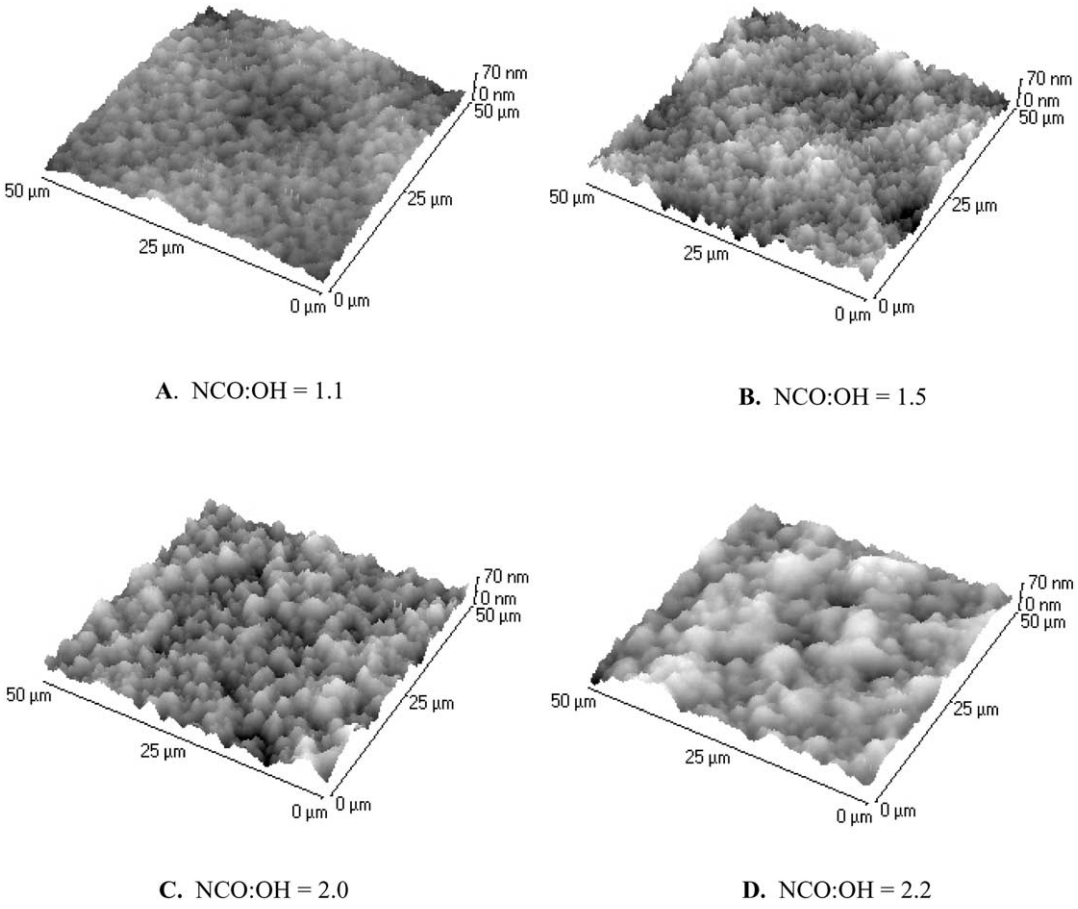

Fig. 3. Topographic AFM images of WB 2K-PUR films crosslinked at 75%RH and 30 °C with varying stoichiometries recorded from the film–air interface.

interface indicates a correlation between PEG content and urea formation at elevated %RH. Consequently, physical stratification of PEG-rich components may enhance urea formation at the F–A interface.

In an effort to verify that water-soluble and mobile components are indeed present in WB 2K-PUR reactive dispersions, a 20 wt% aqueous dispersion of neat WDPI was prepared. Such milky reactive dispersion was allowed to undergo ambient crosslinking for 3 days in the solution state, at which time a small fraction of the dispersion (approx. 0.5 ml) was passed through a nylon membrane syringe filter (Millipore Millex®-GN, 0.20 µm pore size,

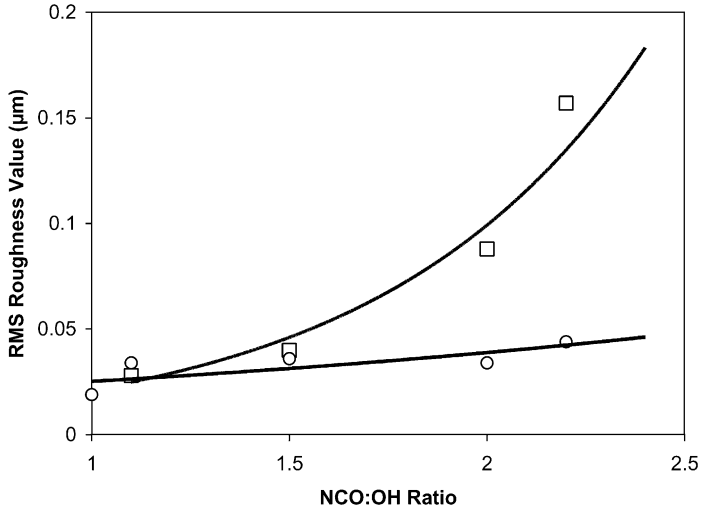

Fig. 4. WB 2K-PUR RMS surface roughness values as a function of NCO:OH ratio: ◇, 82%RH; ○, 75%RH.

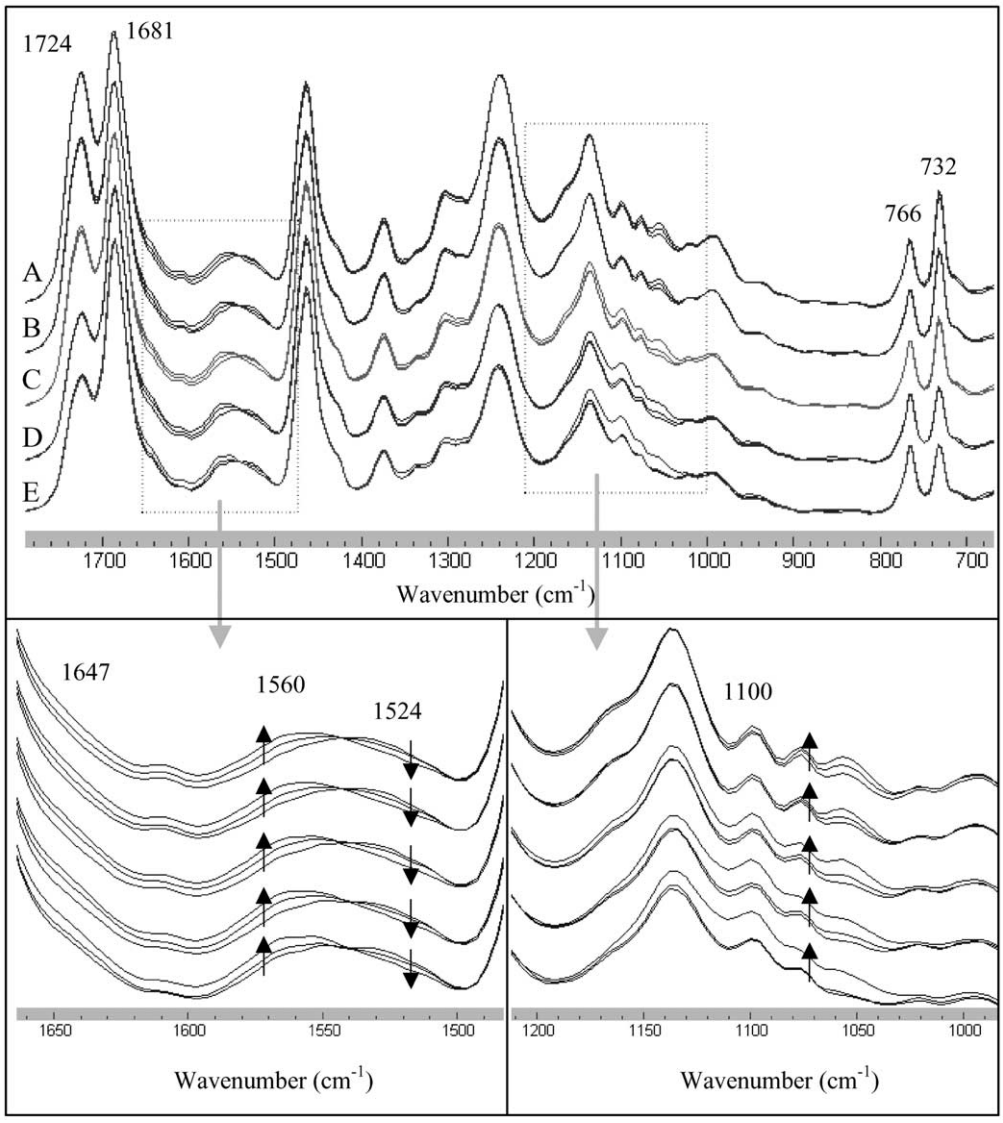

Fig. 5. Overlaid ATR-FTIR spectra of WB 2K-PUR films crosslinked at 30 °C and 32, 52 and 75%RH with varied NCO:OH ratios collected from the film–air (F–A) interface. NCO:OH ratios: (A) 1.0; (B) 1.1; (C) 1.5; (D) 2.0; (E) 2.2. Arrows indicate increasing %RH in each overlaid trace.

4 mm membrane dia.). This approach allows for separation of soluble and insoluble components of the crosslinked network. A completely clear, colorless liquid filtrate was dried at 60 °C overnight, and the isolated solids were subsequently dissolved in DMSO-d_6 for NMR analysis. 500 MHz ^{1}H NMR spectra of the filtrate solids are shown in Fig. 8, Trace A along with the spectrum of neat WDPI in Trace B. As seen, both spectra display a sharp singlet at 3.55 ppm resulting from –(CH_2–CH_2–O)– repeat units of PEG. Furthermore, the 3.55 ppm resonance in Trace A represents the main component of the filtrate, and other peaks associated with WDPI crosslinker only display weak intensities. Consequently, these NMR data verify that water-soluble, mobile components rich in PEG structural units exist in aqueous dispersions containing PEG-modified polyisocyanates. Since enrichment of mobile PEG-containing structural units near the F–A interface is likely responsible for the observed surface morphological features shown in Figs. 2 and 3, we will focus on this aspect in the remaining part of the paper.

In order to correlate morphological features near the F–A and F–S interfaces with chemical changes in WB 2K-PUR films, localized thermal mechanical analysis (LTA) was performed on PUR films that were presumed to have minimal microphase separation (based on their optical clarity). Fig. 9 shows the relationship between T_g and NCO:OH ratio at the F–A and F–S interfaces for 32, 52 and 75%RH films. As shown, the T_g of the F–A ($T_{g,F–A}$) interfacial layer decreases with increasing %RH at each NCO:OH ratio. Furthermore, $T_{g,F–A}$ increases with increasing NCO:OH ratio, as does the F–S T_g ($T_{g,F–S}$), similarly to the MDSC data shown in Fig. 1. However, $T_{g,F–S}$ does not change as much as a function of RH at a given NCO:OH ratio as is the case with the F–A interfacial layer

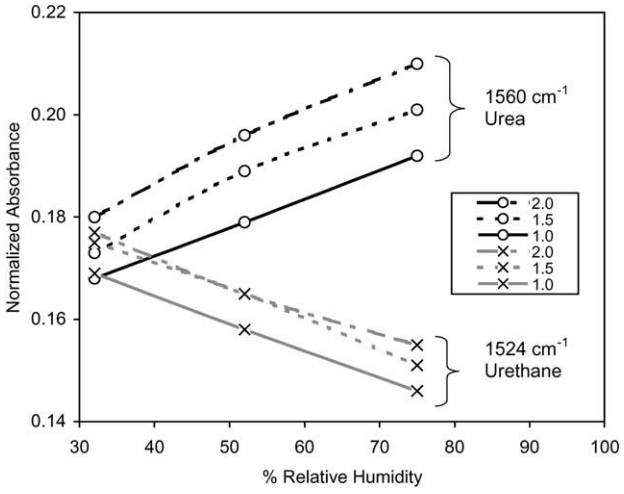

Fig. 6. ATR-FTIR spectral absorbance profiles for 1524 and 1560 cm^{-1} N–H bending modes of WB 2K-PUR films with varied NCO:OH ratios recorded from the F–A interface.

measurements. Additionally, $T_{g,F-A}$ values are significantly higher than $T_{g,F-S}$ values for 32 and 52%RH for all NCO:OH ratios examined, but for 75%RH, $T_{g,F-A}$ is lower than $T_{g,F-S}$. Interestingly enough, the specimen crosslinked at 75%RH results in hazy film appearance at all NCO:OH ratios, and was shown to have PEG enrichment near the F–A interface. Since 75%RH does result in the onset of haze formation and microscopically rough surfaces at NCO:OH ratios of 2.0 and 2.2, such surfaces likely contain microphase separated domains near the F–A interface. These findings are consistent with our previous studies [17,18], and these data indicate that reaction-induced stratification occurs in the films resulting from humidity variations during crosslinking, as thermal property differences exist between the F–A and F–S interfaces.

Fig. 10 shows simultaneously collected topographical and thermal conductivity images recorded from WB 2K-PUR films crosslinked at 82%RH and 30 °C with an NCO:OH ratio of 2.2, which exhibits the roughest surface texture (Fig. 2, D). As seen, there appears to be a correlation between surface topography and relative thermal conductivity (TC), indicating that different surface features exhibit different chemical and/or physical properties. In an effort to ascertain whether or not such physical property differences indeed exist, numerous LTA measurements were performed on both 'hill' and 'valley' regions of the films from three separate areas. A mean hill T_g of 47 °C ($\sigma = 3.5$ °C) and a mean valley T_g of 41 °C ($\sigma = 3.4$ °C) is observed, thus showing that hills and valleys exhibit different thermal properties.

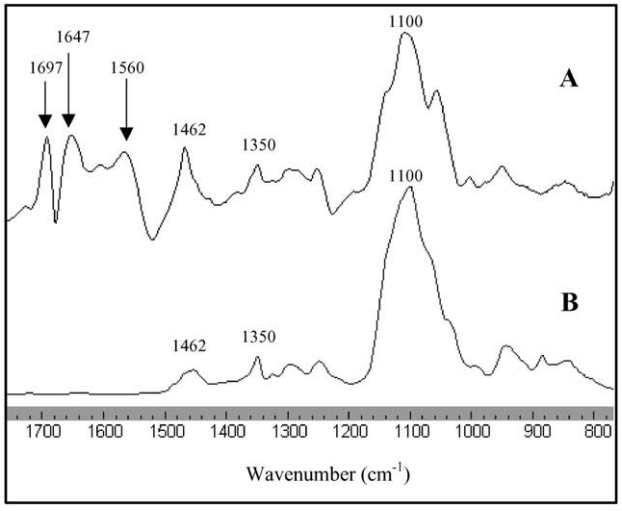

Fig. 7. ATR-FTIR spectra of (A) difference spectrum of NCO:OH = 2.2, (75%RH–52%RH), and (B) PEG, $M_n = 400$ g/mol.

Taking into account the findings of these studies, we are now in a position to formulate a mechanism explaining the formation of surface topographical features on WB 2K-PUR films crosslinked under high RH conditions. First, let us consider the drying process of WB 2K-PUR reactive dispersions. Upon application, a uniform thin layer of reactive dispersion containing approx. 50% water begins to concentrate and thicken, as water rapidly evaporates until an equilibrium water content in the reacting film can be formed with the surroundings. However, the rate of water evaporation is controlled by several factors, including ambient RH, temperature, and hydrophilicity of reactive components. Consequently, high %RH conditions retard evaporation of water such that longer times are required to achieve an equilibrium water content in the film, which increases with increasing %RH. Additionally, the evaporation rate of water during film formation could have a profound effect on the equilibrium shown in Fig. 11, which depicts solution phase surface-bound and unassociated PEG-modified WDPI crosslinkers. Such an equilibrium will be affected by numerous parameters such as time, temperature, PEG molar mass, pH, [WDPI], and droplet size, to name a few. For example, high MW fractions of PEG may render some crosslinker units too hydrophilic to effectively participate in stabilization of non-functionalized polyisocyanate droplets, as they would preferentially partition into the aqueous phase. Furthermore, the presence of multi-functional PEG-modified polyisocyanates (e.g. HDI trimers with 2 or 3 covalently linked PEG chains) in the WDPI should not be ruled out, and likely exists as highly hydrophilic, essentially inert 'crosslinkers' having no reactive isocyanate groups. These entities are also capable of migrating to the F–A interface along with the flux of water when film formation occurs during high humidity conditions. While this is shown in Fig. 11, the question regarding why PEG structural units stratify in WB 2K-PUR films at high RH, but not at low RH still needs to be addressed.

Since concentration gradients of water may exist within the crosslinking film, and rapid water evaporation occurs more rapidly near the F–A interface, low humidity crosslinking conditions will cause reactants to concentrate more rapidly at shallow depths from the F–A interface.

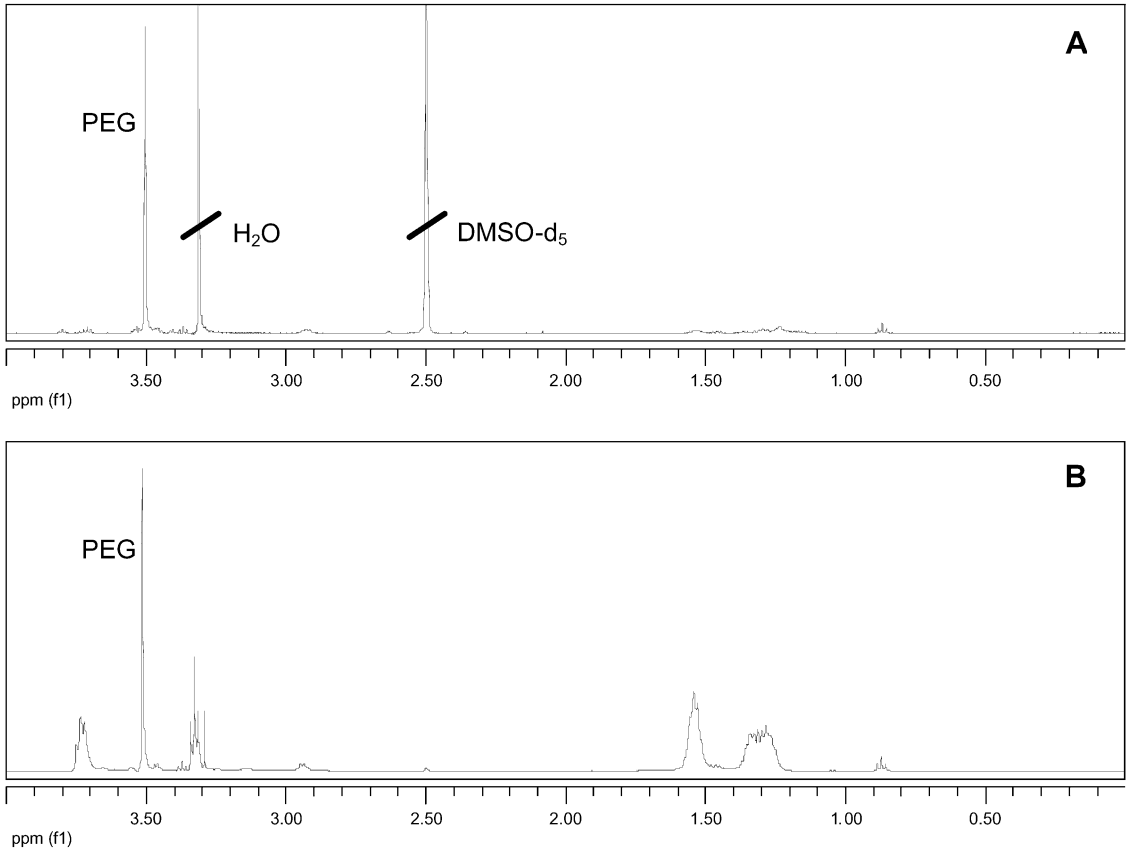

Fig. 8. 500 MHz ^{1}NMR spectra of (A) PEG-rich water-soluble solids from homopolymerized WDPI aqueous dispersion filtrate; (B) neat WDPI.

Subsequently, faster reaction rates, higher viscosity, and decreased ability of diffusants and/or surface-active species to propagate to the F–A interface are anticipated. Such a scenario explains why there is no PEG enrichment near the F–A interface when crosslinking occurs at low RH. Furthermore, the existence of concentration gradients of water should ultimately lead to reaction-induced stratified crosslink density in films (as was shown in Fig. 9), since crosslinking reactions are affected by the presence of water.

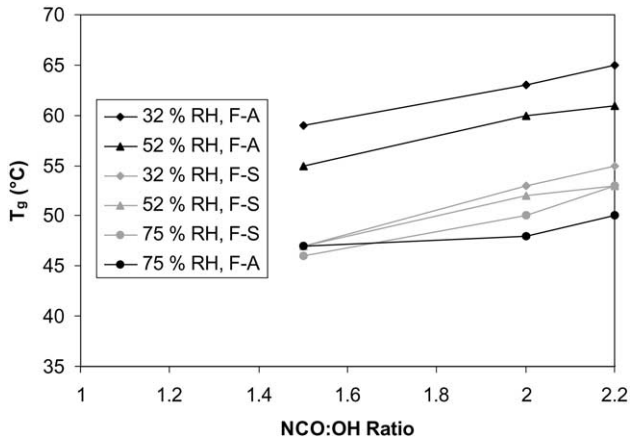

Fig. 9. Average localized thermal analysis data for film–air (F–A) and film–substrate (F–S) interfaces of WB 2K-PUR films.

On the other hand, high RH conditions should result in more uniform concentrations of water across the thickness of the crosslinking film, since water evaporation is slowed overall, particularly near the F–A interface. Also, if the water content of the reactive film is higher, greater mobility of reactants is expected due to hydroplasticization, subsequently delayed mixing of reactants, and slowed crosslinking, leading to the facile diffusion of hydrophilic or surface-active components to the F–A interface along with water.

Fig. 12 shows a model for WB 2K-PUR film formation in which two stages are illustrated for high and low RH conditions. Film formation begins from a wet film having approx. 50% water, which is rapidly lost during the first hour of the process. This regime is denoted ‘Stage I’ and is characterized primarily by the large amount of water lost from the film in a short time. During Stage I, RH determines not only the rate at which water is lost from the film, but also the initial equilibrium water content, $[H_2O]_{eq}$, of the crosslinking film upon entering ‘Stage II’ of film formation, which subsequently takes place from approx 1 to 72 h. For high RH, $[H_2O]_{eq}$ is higher than $[H_2O]_{eq}$ under low RH, and in both cases, $[H_2O]_{eq}$ will be determined by the dynamic equilibrium existing between water in the film and in the surroundings. The $[H_2O]$ at high RH is relatively uniform across the film thickness, since water loss from the F–A

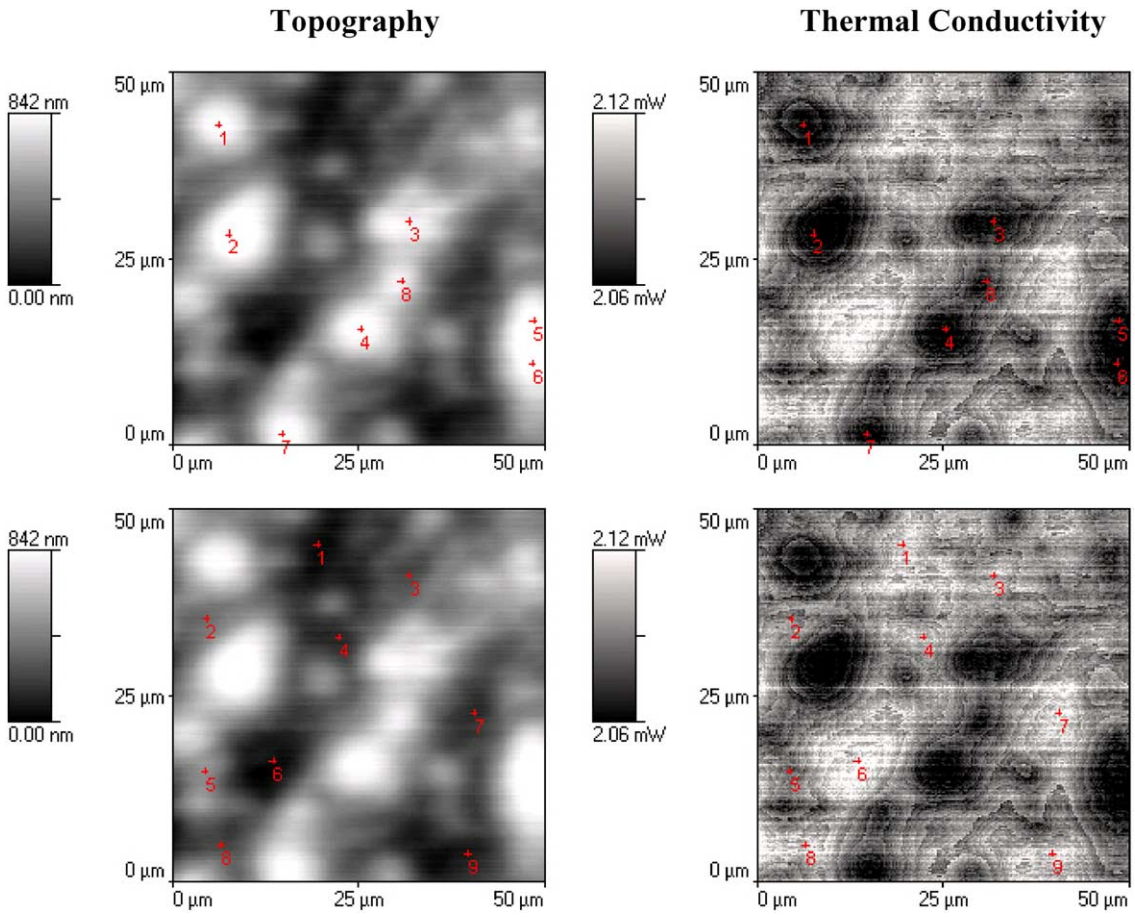

Fig. 10. Representative SThM image of WB 2K-PUR film crosslinked at 82%RH and 30 °C with NCO:OH = 2.2, recorded from the F–A interface with corresponding LTA analysis points indicated.

interface occurs at a rate slow enough to inhibit the development of a concentration gradient. This results in films with relatively evenly distributed crosslink density across the film thickness. Furthermore, the relatively high [H_2O] in the film facilitates diffusion and migration of mobile PEG-rich entities to the F–A interface. Accumulation of PEG-rich structures near the F–A interface results in spinodal decomposition and phase separation of such incompatible moieties coupled with nucleation and growth of surface defects, leading to observed rough surface morphologies. On the other hand, low RH conditions will result in the formation of concentration gradients of water, since water is lost more rapidly near the F–A interface than near the F–S interface. This behavior facilitates the

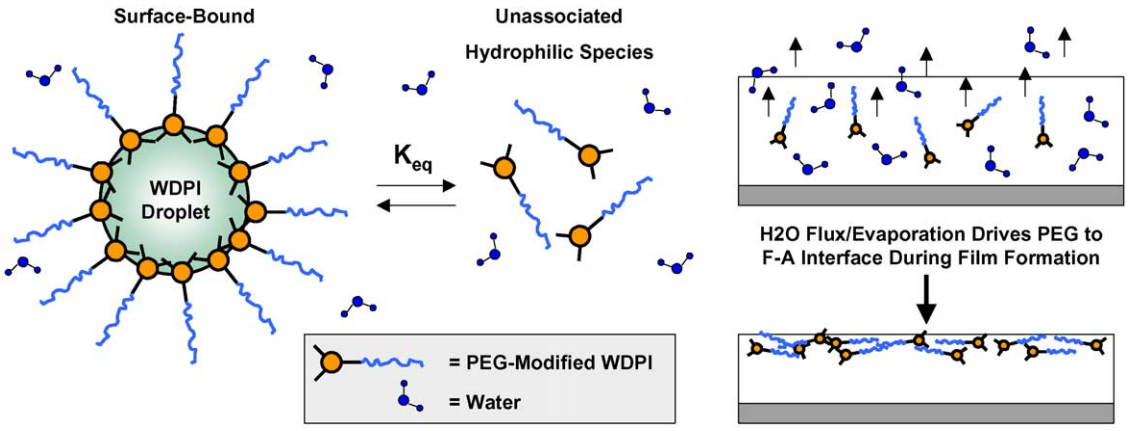

Fig. 11. Schematic illustration of solution behavior of PEG-modified WDPI crosslinkers and their role in producing stratified WB 2K-PUR films.

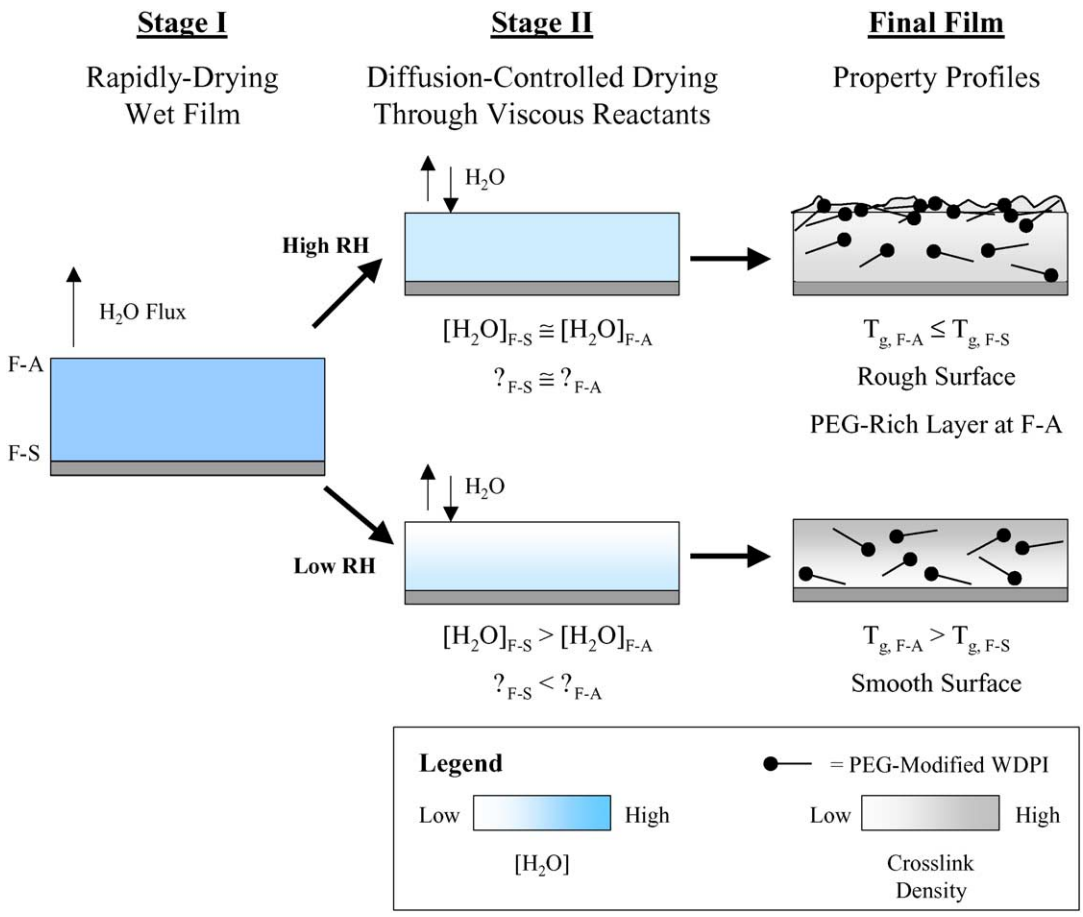

Fig. 12. Schematic diagram of film formation process of WB 2K-PUR films crosslinked under high and low humidity conditions.

development of a layer of reactant material near the F–A interface, which has a higher viscosity than the rest of the film. Consequently, such a viscous layer has low water content, and will undergo accelerated urethane-forming crosslinking reactions near the F–A interface, resulting in stratified crosslink density in the final film. Furthermore, due to the overall lower [H_2O] at low RH, any otherwise mobile species present in the film will be incapable of migrating to the F–A interface, since their diffusivity is greatly reduced. The end result is a relatively homogeneous layer of material near the F–A interface having no phase separation and a smooth topography.

4. Conclusions

These studies underscore the inherent complexity of WB 2K-PUR systems while showcasing the wide range of physico-chemical surface and bulk properties that may be achieved by altering reaction conditions, namely stoichiometry and RH. Specifically, increased humidity and/or NCO:OH ratio may be used to increase surface roughness, which affects film appearance. Furthermore, stratification in such systems occurs as a result of hydrophilic modification of polyisocyanate crosslinkers, leading to enrichment of PEG-containing moieties near the F–A interface and decreased $T_{g,F-A}$ values as a function of increased RH. While low RH conditions generally produce smooth films with a glossy appearance, stratification occurs in such films as well, which was manifested by a T_g difference between F–A and F–S interfaces, which becomes evident at lower RH. It was also shown that T_g differences can exist between microscopic surface 'hills' and 'valleys' of films with high NCO:OH ratio crosslinked at high RH. In essence, these observations paint a three-dimensional picture of the film formation process of WB 2K-PUR coatings in which the governing variable controlling most, if not all, of the film properties, is water.

Acknowledgements

The authors thank Bayer Corporation for donating their starting materials. A partial support from the National Science Foundation Materials Research Science and Engineering Center (MRSEC) Program (DMR 023883) is also acknowledged.

References

[1] Li W, Ryan AJ, Meier IK. Macromolecules 2002;35:5034–42.
[2] Aneja A, Wilkes GL. Polymer 2003;44:7221–8.
[3] Garrett JT, Siedlecki CA, Runt J. Macromolecules 2001;34:7066–70.
[4] Kim Y-S, Lee J-S, Ji Q, McGrath JE. Polymer 2002;43:7161–70.
[5] Ming W, Tian M, van de Grampel RD, Melis F, Jia X, Loos J, et al. Macromolecules 2002;35:6920–9.
[6] Game P, Sage D, Chapel JP. Macromolecules 2002;35:917–23.
[7] Kim JH, Kim SC. Macromolecules 2003;36:2867–72.
[8] Grandy DB, Hourston DJ, Price DM, Reading M, Silva GG, Song M, et al. Macromolecules 2000;33:9348–59.
[9] Rightor EG, Urquhart SG, Hitchcock AP, Ade H, Smith AP, Mitchell GE, et al. Macromolecules 2002;35:5873–82.
[10] Dvorchak M. J Coat Tech 1997;69:47–52.
[11] Feng SX, Dvorchak M, Hudson KE, Renk C, Morgan T, Stanislawczyk V, et al. J Coat Tech 1999;71:51–7.
[12] He ZA, Blank WJ, Picci-King ME, Picci E. J Coat Tech 2002;74: 31–6.
[13] Hegedus CR, Gilicinski AG, Haney RJ. J Coat Tech 1996;68:51–61.
[14] Jacobs PB, Yu PC. J Coat Tech 1993;65:45–50.
[15] Kaminski AM, Urban MW. J Coat Tech 1997;69:113–21.
[16] Melchiors M, Sonntag M, Kobusch C, Jurgens E. Prog Org Coat 2000; 40:99–109.
[17] Otts DB, Urban MW. Polym Prepr 2003;44:105–6.
[18] Otts DB, Urban MW. Proceedings of the international waterborne, high-solids, and powder coatings symposium. vol. 30 2003 p. 365–74.
[19] Otts DB, Urban MW. Polym Mater Sci Eng 2003;88:463–4.
[20] Urban MW, Allison CL, Finch CC, Tatro BA. J Coat Tech 1999;71: 75–85.
[21] Yang J-E, Kong J-S, Park S-W, Lee D-J, Kim H-D. J Appl Polym Sci 2002;86:2375–83.
[22] Barrere M, Landfester K. Macromolecules 2003;36:5119–25.
[23] Lewandowski K, Krepski LR, Mickus DE. J Appl Polym Sci 2004;91: 1443–9.
[24] Wicks ZW, Wicks DA, Rosthauser JW. Prog Org Coat 2002;44: 161–83.
[25] Laas H-J, Halpaap R, Wamprecht C. US Patent 6,426,414, 2002.
[26] Urban MW. Attenuated total reflectance spectroscopy of polymers: theory and practice. Washington. Washington, DC: American Chemical Society; 1996.
[27] Otts DB, Zhang P, Urban MW. Langmuir 2002;18:6473–7.
[28] Public domain software; www.rsb.info.nih.gov.
[29] Rosen SL. Fundamental principles of polymeric materials. 2nd ed. New York: Wiley; 1993.
[30] Silverstein RM, Webster FX. Spectrometric identification of organic compounds. 6th ed 1997.
[31] Wang S-K, Sung CSP. Macromolecules 2002;35:883–8.
[32] Wang S-K, Sung CSP. Macromolecules 2002;35:877–82.